ELECTRICAL ENGINEERING AND ENERGY

OPEN ACCESS

Improving Performance of Squirrel Cage Induction Motor Used in Submersible Pumps

Mümtaz Mutluer[1]

[1] Dept. of Electrical-Electronics Engineering, Konya Technical University, Konya, Türkiye

Submitted: 8 August 2025
Accepted : 19 August 2025
Online First: 22 August 2025

Corresponding author
Mümtaz Mutluer,
mmutluer@ktun.edu.tr

DOI:10.64470/elene.2025.1008

Copyright, Authors, Distributed under Creative Commons CC-BY 4.0

Abstract: This study examines the design of a three-phase induction motor used in submersible pumps. The motor considered is a 380V, 50Hz, 75Hp, 2-pole, 8" three-phase induction motor. The targeted induction motor performance is high efficiency at the rated load. Furthermore, the operating characteristics of the three-phase induction motor, such as starting current, starting torque, breakdown current, breakdown torque, rated current, rated torque, and magnetic flux distribution, were also investigated. The design process began with determining the general geometry of the motor and continued with the calculation of the stator, rotor, and equivalent circuit parameters. Geometric and magnetic constraints were considered during the design process, and priority was given to ensuring that the motor achieves the desired high performance. The motor design simulation was first performed in the Ansys RMxprt module, and then the motor design was simulated in the Ansys Maxwell 2D module and compared with motors from various manufacturers. The resulting motor design geometry has a 4% higher efficiency. Other performance outputs of the motor are also found to be sufficient.

Keywords Ansys, Design, Induction Motor, Submersible Pump.

1. Introduction

Today, electric motors with different design architectures and operating characteristics are studied in academic settings and used in industry (Yücel et. al. 2025; Yücel et. al. 2025; Ünlükaya et. al. 2014; Samur & Altıntaş, 2020). When these motors are classified according to their most general characteristics, it is possible to state that they are asynchronous (induction) and synchronous. Similarly, from a general perspective, induction motors are more cost-effective, more durable, and require less maintenance due to their operating characteristics and design architecture. Commonly used in a wide variety of sectors, induction motors are also widely used in submersible pumps due to these superior features. Although permanent magnet synchronous motors are used in submersible pumps, three-phase induction motors are more commonly used. Therefore, a small increase in the efficiency of induction motors used in submersible pumps will result in significant overall energy efficiency.

Considering the usage dimensions and operating conditions of induction motors used in submersible pumps, it is obvious that there will be some differences from the classical induction motor design. For

example, since the operating environment is underground and in contact with water, it is possible to expect the temperature resulting from motor losses to be not too high (30-35°C) (https://www.polmot.com.tr/tr; https://tr.ferat.com.tr/index.php). This is particularly important in the selection of winding cross-sections. On the other hand, due to the size of the operating environment in submersible pumps, motor diameters are smaller (4", 5", 6", 7", 8", 9", 10", and 12") than in induction motors with similar characteristics, increasing the motor package length to ensure sufficient power density (https://www.polmot.com.tr/tr; https://tr.ferat.com.tr/index.php). These and similar operating characteristics directly affect the design and operating performance of induction motors used in submersible pumps. When the designs of induction motors are examined, it is seen that increasing motor efficiency is at the forefront (Yücel et. al. 2025; Tumbek et. al. 2025). Furthermore, goals such as directly or indirectly achieving high starting torque, low starting current, high rated torque, improving the torque/speed characteristic curve, and reducing cost are also identified (Ergene et. al. 2012; Lee et. al. 2013; Marfoli et. al. 2020; Çunkaş, 2012). In some studies, stator geometry, rotor geometry, and material selection used in the motor are modified, or manufacturing technologies such as die-cast rotor bars are suggested (Manoharan et. al. 2011; Kirtley, 2004). Simulations in these studies are generally performed with finite element method-based programs such as Ansys, Flux, and FEMM (Yücel et. al. 2025; Yücel et. al. 2025; Tumbek et. al. 2025, Ergene et. al. 2012; Arslan, 2016; Galindo et al. 2002). While experimental comparisons are made in studies (Arslan, 2016), most studies prefer to compare simulation results with existing motors.

Induction motor design studies for submersible pumps are rarely single-phase (Gundale & Kulkarni, 2012). Most studies focus on motors below 10HP. Studies focusing on changing the selection and geometry of rotor bars are particularly prominent. In general, ideal conditions are sought in induction motor design studies. However, the torque vibrations of the induction motor and the unbalanced currents in the stator windings were investigated for unbalanced voltages (Donolo et. al. 2011). Studies on the design of three-phase induction motors used in submersible pumps are not very common (Çunkaş, 2012). Therefore, in this study, the design of an 8" diameter, 75Hp three-phase induction motor used in submersible pumps was implemented. The design was simulated with Ansys RMxprt and Maxwell 2D programs and compared with operating values from various companies. According to the results, motor efficiency increased by approximately 4%.

2. Materials and Methods

Certain quantities must be determined at the outset for induction motor design. These include nominal power, synchronous speed, line supply voltage, frequency, and number of phases. Determining Esson's constant, based on the air gap apparent power, is critical in induction motor design (Figure 1) (Boldea & Nasar, 2010). Using Esson's constant in Equation 1, stator internal diameter and package length of the induction motor can be calculated. Based on this general geometry, other geometric calculations for the stator and rotor can be made.

$$D_{is} = \sqrt[3]{\frac{2p_1}{\pi\lambda}\frac{p_1}{f_1}\frac{S_{gap}}{C_0}} \quad (1)$$

where, p_1 is the number of poles, λ is the package aspect ratio, f_1 is the frequency, S_{gap} is the air gap apparent power in kVA, and C_0 is the Esson's constant in J/dm^3 (Boldea & Nasar, 2010).

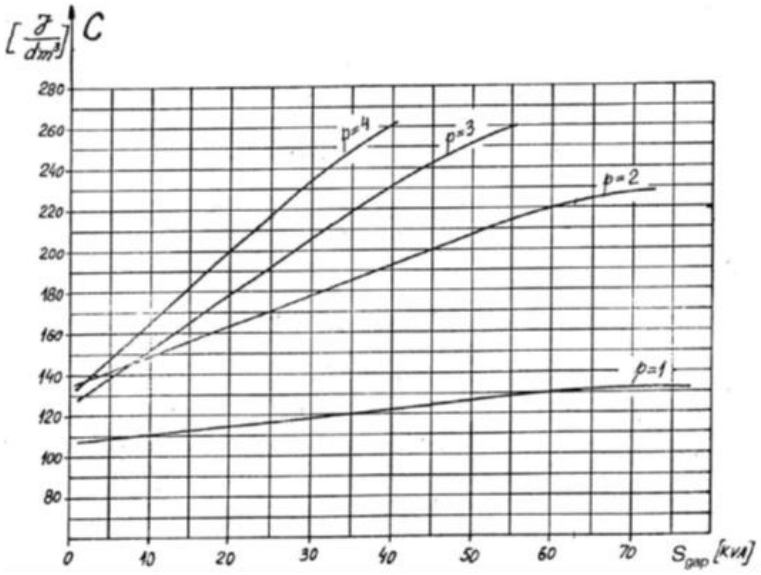

Figure 1 Esson's constant graphs versus S_{gap} air gap apparent power

In induction motor design, consideration should be given to the calculation of two important design parameters beyond geometry. The first of these is the stator winding quantity and its cross-section. While the stator winding quantity depends on many parameters, the most important factor is the air gap flux. The winding quantity is calculated using the air gap flux selected according to Table 1, and the winding cross-section is related to rated current of the motor and the net usable area of the stator slot.

Table 1 Air gap flux density according to pole number

Pole number ($2p_1$)	Air gap flux density (B_g) (T)
2	0.5-0.75
4	0.65-0.78
6	0.7-0.82
8	0.75-0.85

The second most influential design factor is the rotor slot shape and material. The rotor slot shape determines torque/speed curve and efficiency of the motor by changing the rotor resistance and reactance ratio throughout the operating range, from startup to synchronous speed. Aluminum is generally the preferred rotor slot material for low-power machines, while copper is preferred for high-power machines. Furthermore, die-casting the rotor bar also increases efficiency and reduces operational failures (Manoharan et. al. 2011; Kirtley, 2004).

Today, the use of commercial finite element-based software is indispensable in electrical machine studies. One of the most popular of these programs is Ansys. Because the features offered by the Ansys RMxprt and Maxwell modules are very practical and useful, designers can quickly simulate their work, easily transfer the analytical design to the magnetic analysis platform, and perform more detailed analyses. The stator and rotor slot shapes presented in the Ansys RMxprt module are shown in Figure 2. Slot dimensions can be entered by selecting any of these geometries. After analytical simulation, the motor can be transferred to the 2D or 3D Maxwell module with all its design parameters. 2D geometry is generally preferred due to data size and processing time. With the Ansys Maxwell module, outputs such as magnetic flux distribution and torque-speed curve of the motor can be provided with higher precision.

a)

b)

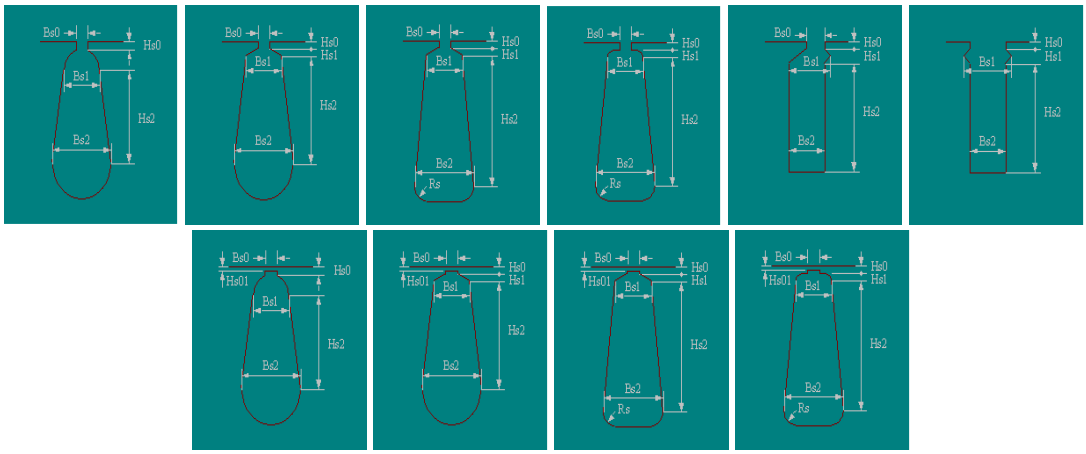

Figure 2 Ansys RMxprt a) stator slot shapes b) rotor slot shapes

The input parameters of the induction motor designed for 8" submersible pumps in this study are given in Table 2. Design details can be examined from various sources (Boldea & Nasar, 2010).

Table 2 Design parameters of the three-phase induction motor

Design parameters	Unit	Value
Rated power	kW	55
Synchronous speed	rpm	3000
Supply voltage	V	380
Frequency	Hz	50
Phase number	–	3
Pole number	–	2
Steel sheet	–	M19-24G
Stator/Rotor conductor	–	Copper

3. Results and Discussion

The power/speed, torque/speed, current/speed and efficiency/speed graphs of the three-phase induction motor obtained with Ansys RMxprt are given in Figure 3. The nominal efficiency of the motor is 89.3%, the nominal speed is approximately 2890 rpm, the nominal torque is 182.26 Nm and the nominal current is 101.75 A. According to these results, motor efficiency has increased by approximately 4% (https://www.polmot.com.tr/tr; https://tr.ferat.com.tr/index.php).

a)

b)

c)

d)

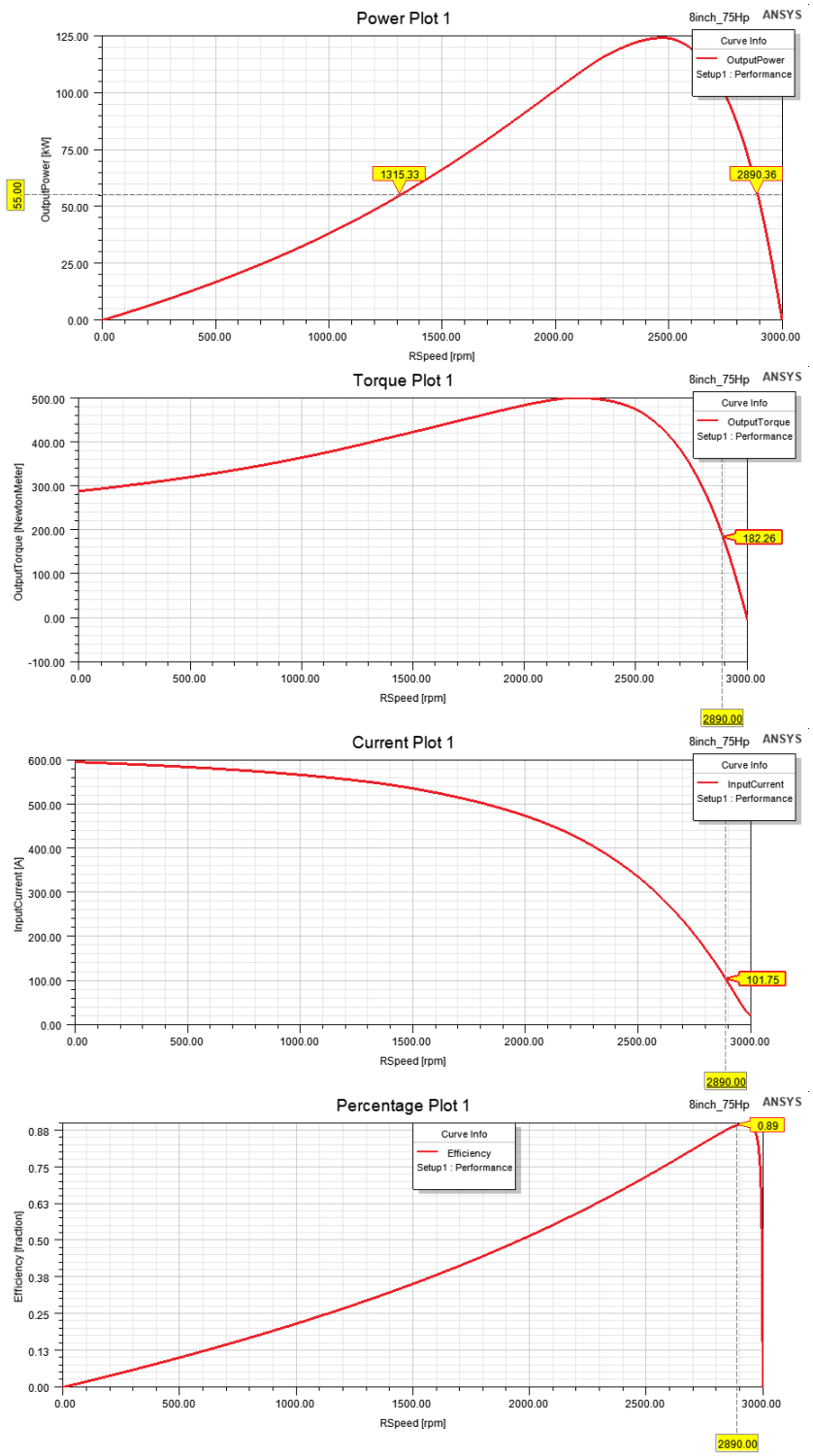

Figure 3 Ansys RMxprt graphics **a)** power/speed **b)** torque/speed **c)** current/speed **d)** efficiency/speed

After the analytical simulation was performed, the rated values of the induction motor were taken as the basis and transferred to Ansys Maxwell 2D. As a result of the simulations performed with Ansys Maxwell 2D, the input power/time graph, output power/time graph, torque/time graph, current/time graph and magnetic flux density graph of the three-phase induction motor are given in Figure 4. In the graphs in

Figure 4, the average and effective values are labeled for the 100ms-180ms interval. In general, the analytical and numerical simulation results of the induction motor are consistent with each other. Furthermore, the magnetic flux density values are within acceptable limits. Some important design outputs for the motor and the operating values from various manufacturers (https://www.polmot.com.tr/tr; https://tr.ferat.com.tr/index.php) are given in Table 3. According to Table 3, the three-phase induction motor designed for the submersible pump provides satisfactory performance in terms of operating values.

a)

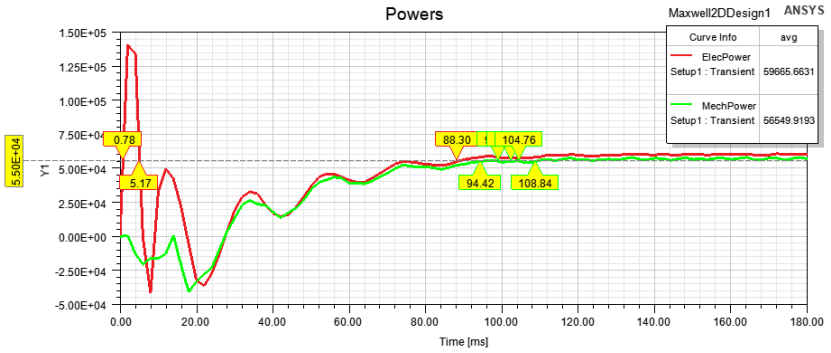

b)

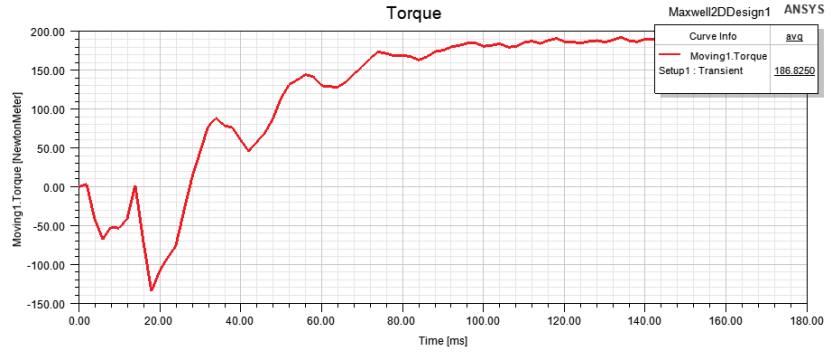

c)

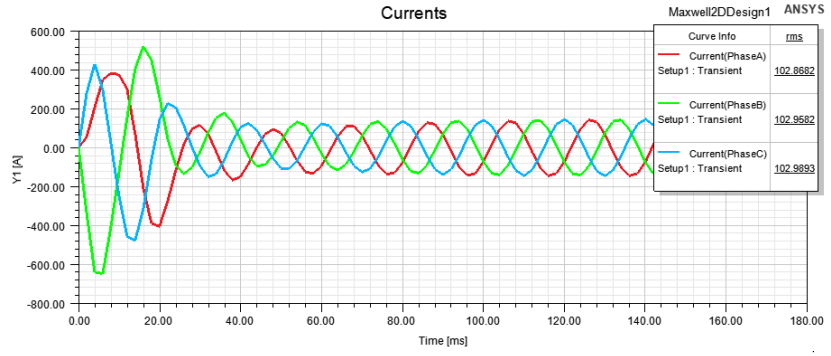

d)

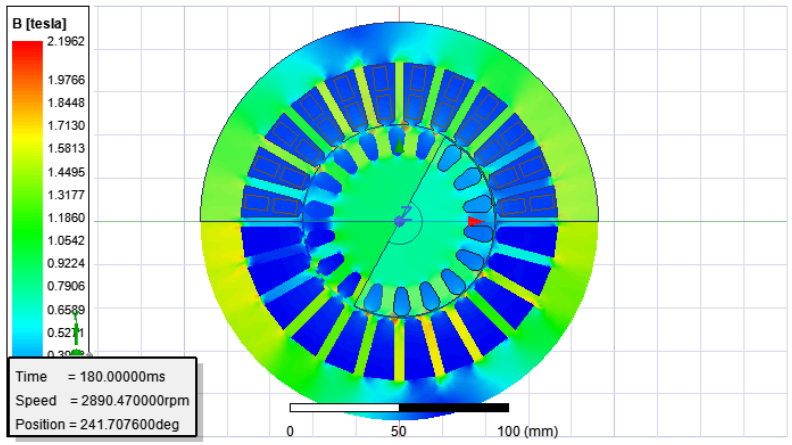

Figure 4 Ansys Maxwell 2D graphics **a)** input power/time, output power/time **b)** torque/time **c)** current/time **d)** magnetic flux density

Table 3 Design outputs of the three-phase induction motor

Design outputs	Unit	Value		
		IM	POLDAP (HPL875/1A) (https://www.polmot.com.tr/tr)	FERAT (FM8/75) (https://tr.ferat.com.tr/index.php)
Output power	kW	55	55	55
Input power	kW	61.6	–	–
Efficiency	%	89.3	86	85.7
Rated speed	rpm	2890.47	2885	2883
Power factor		0.915	0.87	0.86
Start-up torque	Nm	287.7	–	–
Break-down torque	Nm	499.3	–	–
Rated torque	Nm	181.7	–	–
Start-up current	A	595	–	624
Break-down current	A	426.3	–	–
Rated current	A	101.4	112	114
Stator tooth magnetic flux	T	1.56	–	–
Stator yoke magnetic flux	T	1.54	–	–
Rotor tooth magnetic flux	T	1.56	–	
Rotor yoke magnetic flux	T	0.94	–	–

This study was conducted for an 8", 75Hp, three-phase induction motor used in submersible pumps. Because operating conditions and production criteria were neglected for the design, some aspects of the study reflect ideal conditions. Furthermore, implementing the motor design using one of the known optimization methods, such as genetic algorithm, particle swarm algorithm, gray wolf algorithm, etc., would make the results more useful and improve the study in many ways.

In the design of induction motors, design classes are formed, particularly based on rotor bar geometry (Boldea & Nasar, 2010; Chapman, 2004). This factor, which guides the design at the beginning, should be reviewed at the end. Examining the data obtained in Table 3 for the motor designed in this study, the starting torque to rated torque ratio is 1.58, the breakdown torque to rated torque ratio is 2.75, the starting current (short-circuit current) to rated current ratio is 5.87, and the nominal slip is 3.65%. These values correspond to design class B in NEMA standards.

4. Conclusions

This study conducted the design and simulations of a 380V, 50Hz, 75Hp, 2-pole, 8" three-phase induction motor used in submersible pumps. The results revealed a model with 4% higher efficiency compared to motors from various manufacturers. Graphs for torque, power, current, efficiency, and magnetic flux density of the motor are also presented. The graphs indicate that the nominal operating values of the motor are sufficiently large. The primary power loss of the motor is due to stator copper losses. Therefore, it would be appropriate to optimize the design of the induction motor in this direction.

Declaration of Ethical Standards

As the author of this study, I declare that he complies with all ethical standards.

Credit Authorship Contribution Statement

M.Mutluer: Investigation, Resources, Design, Software, Validation, Formal analysis, Writing-Original Draft, Visualization, Review & Editing, Supervision.

Declaration of Competing Interest

The author declared that they have no conflict of interest.

Funding / Acknowledgements

No project support was received.

Data Availability

No datasets were generated or analyzed during the current study.

References

Yücel, E., Karabulut, C., & Çunkaş, M. (2025). Design, implementation, and testing of a propulsion system for the hyperloop transportation system. Electrical Engineering, 1-21.

Yucel, E., Cunkas, M., & Knypiński, Ł. (2025). Evaluation of magnet demagnetization behavior in permanent magnet linear synchronous motors. Electrical Engineering and Energy, 4(1), 52-63.

Ünlükaya, E., Yetkin, A. G., Çanakoğlu, A. İ., & Turan, M. (2014). Rotor oluk şekillerinin asenkron motor performansına etkileri. Eleco 2014 Elektrik–Elektronik–Bilgisayar ve Biyomedikal Mühendisliği Sempozyumu, 27-29.

Samur, K., & Altıntaş, N. (2020). Dalgıç pompa elektrik motorunun iyileştirilmesi. Harran Üniversitesi Mühendislik Dergisi, 5(2), 82-93.

(2025, 8 June), https://www.polmot.com.tr/tr

(2025, 8 June), https://tr.ferat.com.tr/index.php

Tumbek, M., Oner, Y., & Kesler, S. (2015). Optimal design of induction motor with multi-parameter by FEM method. In 2015 9th International Conference on Electrical and Electronics Engineering (ELECO) (pp. 1053-1056). IEEE.

Ergene, L., Şal, S., & İmeryüz, M. (2012). Kafesli asenkron motorlarda maliyet kısıtı altında rotor çubuklarının analizi/The analysis of the squirrel cage induction motor rotor bars under the cost constraint. EMO Bilimsel Dergi, 2(3), 23-28.

Lee, G., Min, S., & Hong, J. P. (2013). Optimal shape design of rotor slot in squirrel-cage induction motor considering torque characteristics. IEEE Transactions on Magnetics, 49(5), 2197-2200.

Marfoli, A., Di Nardo, M., Degano, M., & Gerada, C. (2020). Rotor slot optimization of squirrel cage induction motor. In The 10th International Conference on Power Electronics, Machines and Drives (PEMD 2020) (Vol. 2020, pp. 972-977). IET.

Çunkaş, M. (2012). Dalgıç motorlar üzerine bir inceleme. Selçuk Üniversitesi Mühendislik, Bilim Ve Teknoloji Dergisi, 27(4), 135-148.

Manoharan, S., Devarajan, N., Deivasahayam, M., & Ranganathan, G. (2011). Enriched efficiency with cost effective manufacturing technique in 3.7 kW submersible pump sets using DCR technology. International Journal on Electrical Engineering & Informatics, 3(3).

Kirtley Jr, J. L. (2004). Designing squirrel cage rotor slots with high conductivity. In Proc. of ICEM (Vol. 4).

Arslan, S. (2016). Dalgıç motorun analitik, sayısal, performans sonuçlarının karşılaştırılması. Düzce Üniversitesi Bilim ve Teknoloji Dergisi, 4(2), 403-415.

Galindo, V. A., López-Fdez, X. M., Pinto, J. D., & Coimbra, A. P. (2002). Parametric study of rotor slot shape on a cage induction motor. Studies in applied electromagnetic and mechanics, 22, 190-195.

Gundale, V. A., & Kulkarni, M. S. (2012). A practical approach to the design & implementation of a water cooled single phase submersible motor. Int J of Eng Res & Appl, 2(1), 299-304.

Donolo, P., Bossio, G., & De Angelo, C. (2011). Analysis of voltage unbalance effects on induction motors with open and closed slots. Energy Conversion and Management, 52(5), 2024-2030.

Ion, B., & Syed, A. N. (2010). The Induction Machines Design Handbook. Electric Power Engineering Series, 2nd ed., by Taylor and Francis Group, LLC, Boca Raton London New York.

J Chapman, S. (2004). Electric Machinery Fundamentals.